MAJOR PAPER

Microstrip Transmission Line RF Coil for a PET/MRI Insert

Md Shahadat Hossain Akram[*], Takayuki Obata, and Taiga Yamaya

Purpose: We proposed and developed a new microstrip transmission line radiofrequency (RF) coil for a positron emission tomography (PET) insert for MRI, which has low electrical interactions with PET shield boxes. We performed imaging experiments using a single-channel and a four-channel proposed RF coils for proof-of-concept.

Methods: A conventional microstrip coil consists of a microstrip conductor, a ground conductor, and a dielectric between the two conductors. We proposed a microstrip coil for the PET insert that replaced the conventional single-layer ground conductor with the RF shield of the PET insert. A dielectric material, which could otherwise attenuate gamma photons radiated from the PET imaging tracer, was not used. As proof-of-concept, we compared conventional and the proposed single-channel coils. To study multichannel performance, we further developed a four-channel proposed RF coil. Since the MRI system had a single-channel transmission port, an interfacing four-way RF power division circuit was designed. The coils were implemented as both RF transmitters and receivers in a cylindrical frame of diameter 150 mm. Coil bench performances were tested with a network analyzer (Rohde & Schwarz, Germany), and a homogeneous phantom study was conducted for gradient echo imaging and RF field (B_1) mapping in a 3T clinical MRI system (Verio, Siemens, Erlangen, Germany).

Results: For all coils, the power reflection coefficient was below −30 dB, and the transmission coefficients in the four-channel configuration were near or below −20 dB. The comparative single-channel coil study showed good similarity between the conventional and proposed coils. The gradient echo image of the four-channel coil showed expected flashing image intensity near the coils and no phase distortion was visible. Transmit B_1 field map resembled the image performance.

Conclusion: The proposed PET-microstrip coil performed similarly to the conventional microstrip transmission line coil and is promising for the development of a compact coil-PET system capable of simultaneous PET/MRI analysis with an existing MRI system.

Keywords: *parallel transmission RF coil, microstrip transmission line, PET-strip coil, magnetic resonance imaging, PET insert*

Introduction

For more than two decades, studies on multimodal medical imaging[1–3] have shown immense success in the areas of diagnostic accuracy and therapy monitoring. The integration of computed tomography (CT) with positron emission tomography (PET)[4] or single-photon emission computed tomography[5] has seen vast clinical applications. Specifically, these systems have become common in clinical practice in oncologic and psychiatric studies.[3–7] One of the major reasons for this growing interest in multimodal imaging is to obtain complementary diagnostic information from different systems in a combined single-bed imaging protocol. For example, in a tandem single hybrid PET/CT system, anatomical images of a patient provided by a CT scanner are combined with metabolic images provided by a PET scanner. This hybrid imaging approach improves the accuracy of cancer diagnosis and phenotyping through the analysis of biochemical changes of cancer cells within the anatomical framework of a patient. Nevertheless, CT scanning is conducted before PET scanning in these sequential imaging systems.

Although anatomical MRI has been used in most PET/MRI studies, a hybrid PET/MRI system[7–12] has shown

several potential advantages over the PET/CT and SPET/CT systems: a reduction in radiation exposure from CT,[13,14] simultaneous multimodal imaging, superior soft-tissue contrast by MRI, and functional MRI and magnetic resonance spectroscopic (MRS) imaging by the same MRI system.[7,15] Some studies have recently reported on PET/MRS imaging as well.[16–18] Although the whole-body PET/MRI system became available in 2010,[9] recent growing interest in the development of a low-cost PET insert (such as a brain PET) for existing MRI systems[19–24] has created a potentially dominant new research field in multimodal medical imaging research. However, in all these PET insert developments, a single-channel volume radiofrequency (RF) coil (e.g., birdcage RF coil) was implemented as a transmitter. This approach was required to implement a separate multichannel surface RF coil for high-sensitive RF reception, which is a common clinical imaging practice. From the PET imaging perspective, this approach increases the photon attenuation by the two sets of RF coils. From the RF compatibility perspective, this strategy increases the diameter of the PET ring to provide enough space for the efficient performances of both the transmitting and receiving coils. Moreover, a single-channel transmit RF coil is not feasible for ultrahigh field (UHF) MRI applications, as destructive RF interference dominates at UHF, and a multichannel transmit approach (e.g., transmit SENSE) is the state-of-the-art solution.[25–31]

Conventionally, detectors and front-end electronics of a PET insert are RF shielded to avoid electromagnetic (EM) interference between the two systems.[19–24] In this study, we developed a novel design of a microstrip transmission line RF coil[27–30] that combines the RF shield of a PET detector module with a microstrip conductor that acts as a transmission line coil. The conventional microstrip coil consists of two metal conductors (one is a microstrip conductor, and the other is a ground conductor) and a dielectric between the two conductors.[27] This study considered the RF shield of the PET detectors as the ground conductor for the microstrip coil, which reduces the amount of RF shielding that would otherwise be required if a separate microstrip RF coil is designed for a PET insert for an MRI system. The reduction in RF shield materials is important for a reduced gradient eddy current effect,[32] which is one of the major design challenges for PET insert researchers.[19–25] Moreover, the combined PET-microstrip coil modality should be a compact single multimodal device that can be mounted with ease on an existing patient bed of an MRI scanner similar to the extremity RF coils, such as the head RF coil. Since the combined system is a single PET-coil module with minimal coil components, it should have minimal photon attenuation in the RF coil (e.g., only microstrip conductor) and would provide strong mechanical support. The RF compatibility of the proposed coil should be simpler than that of the conventional two separate RF coil approaches.

Furthermore, a single-channel volume RF coil depends on geometric symmetry that limits the design choice of PET geometry, such as a cylindrical brain PET insert to be used with a cylindrical birdcage RF coil.[19–24] The proposed coil would enable designing asymmetric PET-coil geometries; for example, designing a semioval PET insert to be used above the patient bed for pediatric imaging. It would be suitable for ultrahigh field applications as well. On the other hand, compared with that of the loop coil, the number of coils in the multichannel configuration increases with the microstrip coils that require relatively simple decoupling between the coils.[28,31] An increase in the transmit loop coil elements results in a reduction in loop size that would otherwise reduce the depth sensitivity of each coil.[28] In case of the proposed microstrip coil, the ground plate (here, the PET detector shield box) is part of the coil and can be moved closer to the microstrip conductor.[33] However, for a surface coil, this very close positioning of the PET shield as a separate component would have adverse effects, like the reduction of transmit field homogeneity and a requirement for very high RF power.[34] Moreover, the presence of a B_{1z} component in the surface coil absorbs high levels of RF power and increases power deposition.[33] Furthermore, using the surface transmitting RF coil for the PET insert would be similar to the conventional design approach of separate RF coil and PET insert that requires precise positioning of both modules and would make the system sensitive to mechanical vibration and rotation due to gradient fields.

As a proof of our concept, we first performed a comparative study using two single-channel microstrip RF coils, where one coil was constructed according to the conventional approach and the other coil was constructed according to the proposed approach. Then, we developed a four-channel proposed PET-strip coil to evaluate the multichannel performance. The coils were designed considering our available 3T clinical MRI system (Verio, Siemens, Erlangen, Germany). This study explains the coil design details, its bench performances, and the phantom imaging of a gradient echo (GRE) sequence and the RF transmit (B_1) field response. All coils in this study were implemented as both an RF transmitter and receiver. Previous studies on receive-only multichannel RF coils dedicated for PET/MR studies can be found in the literature.[35,36] To the best of our knowledge, this is the first study focused on the development of a PET insert dedicated to parallel transmit/receive RF coil targeting for PET/MR analysis.

Materials and Methods

Coil design

Following the calculation approach described in Lee et al.,[28] we calculated the design parameters for the conventional microstrip coil, and the design parameters for the proposed coil were estimated based on those values. For more detail on the basics of the microstrip transmission line, interested readers can review the references.[37] A comparative schematic representation of the conventional and proposed coils is shown in Figs. 1a and 1b, respectively. In the proposed coil, the ground conductor (shown in Fig. 1a) was replaced with the
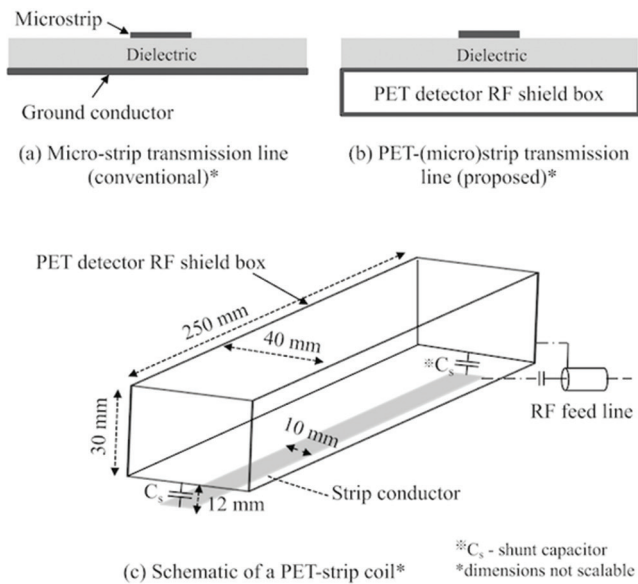
Fig. 1 Schematics of (**a**) the conventional microstrip transmission line; (**b**) the proposed positron emission tomography (PET)-strip transmission line; and (**c**) the RTL design of the PET-strip coil that used two shunt capacitors along the strip to limit the coil length to the axial imaging dimension (250 mm in this study) of interest. The RF shield box of the PET detector module was used as the ground conductor for the proposed microstrip coil. RTL, reduced-length transmission line; RF, radiofrequency.

RF shield of the PET detector module, as shown in Fig. 1c. Although a microstrip transmission line can be constructed with only the microstrip conductor, the ground conductor and dielectric materials, in which the dimensions of these components and their electromagnetic properties can determine the coil resonance frequency and other performance parameters,[27,28] the implementation of multiple shunt capacitors (e.g., Fig. 1c) between the two conductors is required[28–30] to design a coil for the NMR resonance frequency of interest for MRI systems, with the practical consideration of the limited axial length of the targeted imaging region. This type of microstrip transmission line deploying two or more shunt capacitors along the strip is described in Lee et al.[28] as a 'reduced-length transmission line (RTL)'.

For this study, we considered the axial length of the coil to be 250 mm. The other dimensions of the microstrip conductor were a width of 10 mm and a thickness of 35 μm. The width of the ground plane for the conventional coil was selected as 40 mm. The calculated[28] gap between the microstrip and ground conductors to tune the coil to the required resonance frequency was 12 mm. The calculation of the design parameters was performed without consideration of dielectric materials in the gap, which was kept filled with air to avoid possible gamma photon attenuation and scattering in the dielectric materials that would otherwise reduce the sensitivity of the PET images.[19,33,34] The dimensions of the PET detector shield box were selected as $250 \times 40 \times 30$ mm³, as

shown in Fig. 1c. Additionally, 35-μm-thick copper printed circuit board was used as the conducting material for all coil construction. Images of the developed PET-strip coil are shown in Figs. 2a and 2b. There are several opening slits (that were covered by copper mesh) on one end-face of the shield box (left end in Fig. 2a, not shown) for the purpose of air cooling of the PET detector electronics and a 20-mm-diameter opening on the other end-face (right end in Fig. 2a) for access to the PET detector data and power cables inside the shield box. A 0.5-mm-thick aluminum pipe with a length of 20 mm was used on the right end-face to connect the shield box with the PET detector cable shields (e.g., copper tube). An image of the four-channel coil inside the MRI bore is shown in Fig. 2b. Figure 2c shows the PET-strip coil with shunt capacitors implemented in this design. On both ends of the strip, we implemented a parallel combinationn of fixed-value (10 pF) ceramic capacitors and variable trimmer capacitors (1–16 pF). These design values were chosen based on calculations described in Lee et al.[28] and Nelatury et al.[38] The same capacitors were also implemented to design the single-channel conventional microstrip coil.

Multichannel coil interface for the existing one-channel transmit system

All the coils in this study were implemented as both a transmitter and receiver. The four-channel coil was implemented in a cylindrical orientation with an inner diameter of 150 mm and an equal angular distance of 90°. Our 3T MRI system was equipped with a single-channel RF transmission and a 32-channel reception system. For the four-channel PET-strip coil, we developed an interfacing circuit that included a four-way RF power
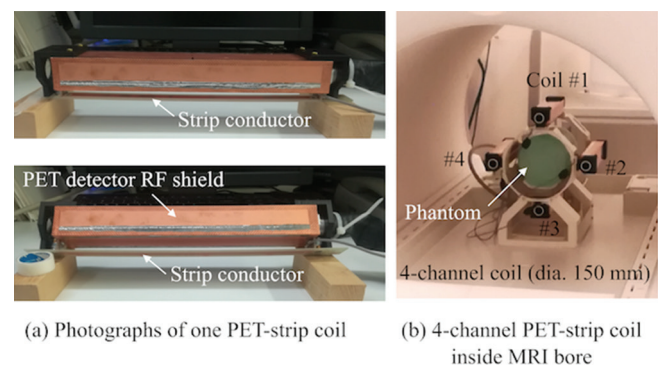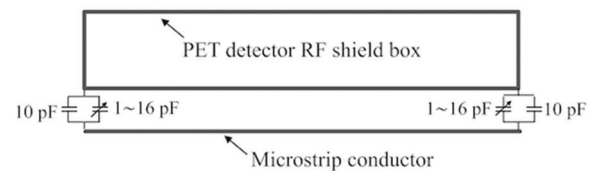
Fig. 2 (**a**) Images of the proposed PET-strip coil. (**b**) The four-channel coil in a cylindrical orientation with an inner diameter of 150 mm. (**c**) A schematic of the proposed coil with shunt capacitors. PET, positron emission tomography.

divider, low noise preamps, and transmit/receive (T/R) switches. A schematic of the interfacing circuit is shown in Fig. 3a. For this study, we developed a customized low-cost 4-way RF power divider capable of a 90° phase shift between the coils using 90° hybrid circuits that are conventionally used with a quadrature mode volume RF coil that splits the single-channel transmit signal from the MRI RF driver to an in-phase (0°) signal and a 90° out-of-phase signal. A schematic representation of the power divider and the phase shifter is shown in Fig. 3b. An interfacing circuit for the comparative single-channel study was developed separately. The coil and the interfacing circuits were manufactured in Takashima Sei-sakusho Co., Ltd., Tokyo, Japan.

Experimental study

For a comparative study between the conventional microstrip coil and the proposed PET-strip coil, GRE images were generated with a homogeneous bottle phantom (NaCl and distilled water solution) with an axial length of 120 mm, a width of 80 mm and a depth of 50 mm. A 200-mm-long and 110-mm-diameter cylindrical homogeneous phantom (per 1000 g distilled water: 3.75 g $NiSO_4 \times H_2O$ + 5 g NaCl) was used to investigate the coil bench performances to generate a GRE image and transmit B_1 field responses of the four-channel coil. GRE images were acquired for the following sequence parameters: TR = 600 ms, TE = 4 ms, slice thickness = 5 mm, flip angle = 30°, image matrix = 128 × 128, transverse FOV for the bottle phantom = 120 mm, transverse FOV for the cylindrical

phantom = 150 mm, and transaxial FOV for the bottle phantom = 150 mm. For B_1 field mapping, separate two-dimensional GRE transverse magnitude images were acquired at 30° and 60° flip-angles and a TR of 3000 ms, with all other parameters similar to those used for the GRE imaging. From the two magnitude images, B_1 field maps were calculated using the double-angle method.[39,40] In the case of a single-channel study, the coronal B_1 field was measured, whereas the transverse B_1 field was measured for a four-channel coil. Moreover, to investigate the effect of the PET cable RF shield on the coil performance, imaging measurements were acquired with the single-channel PET-strip coil for two different orientations of the cable shield connected to the shield box and compared with the results without the cable shield case. PET detector electronics were not included in this study. A network analyzer (Rohde & Schwarz, Germany) was used to tune and match all the coils to 123.22 MHz and 50 Ω. To confirm the RF power transmission coefficients, a 15-mm-diameter pickup coil was used in this study.

Results

Figure 4 shows comparative transverse and sagittal GRE images for the single-channel conventional microstrip and the proposed PET-strip coils. This study was conducted for the coil position on the lower side of the phantom. For both the coils, the reflection coefficient (S_{11}) was approximately −30 dB.
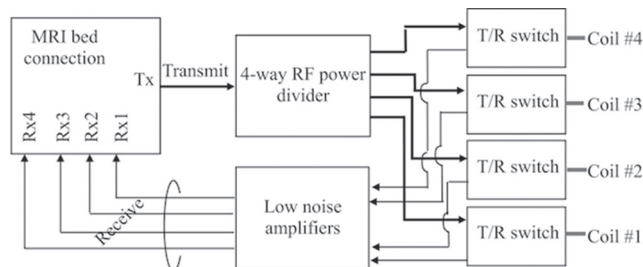

(a) Schematic of the interfacing circuit connecting the 4-channel coil to the MRI system (that is equipped with 1-channel transmit and multichannel receive).
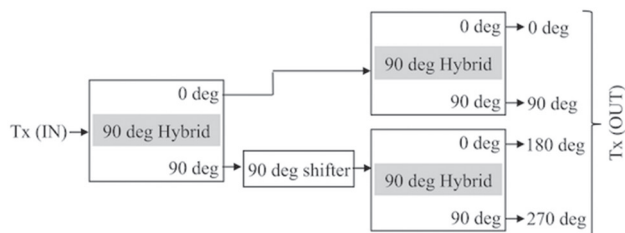

(b) Schematic of the custom-designed 4-way RF power divider shown in figure (a).

Fig. 3 (**a**) A schematic of the interfacing circuit developed to be used with our single-channel transmitter and 32-channel receiver MRI system. (**b**) A schematic of a custom-designed 4-way RF power divider that implements a conventional 90° hybrid for power division to four PET-strip coils. PET, positron emission tomography; RF, radiofrequency.
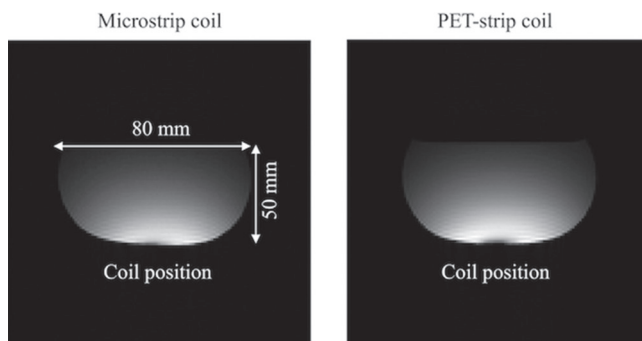
(a) Transverse plane
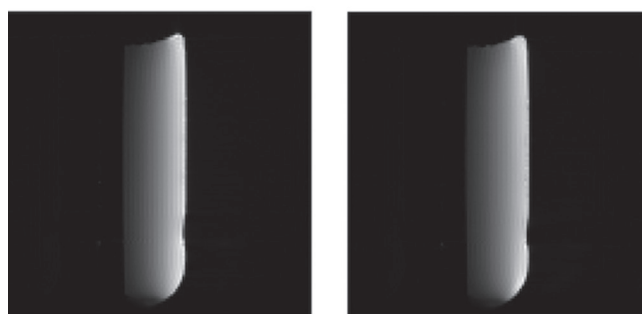
(b) Sagittal plane

Fig. 4 Gradient echo images for the conventional single-channel microstrip coil (left column) and the proposed single-channel PET-strip coil (right column). PET, positron emission tomography.

A comparison of flip-angle line profiles in the axial direction is shown in Fig. 5a. Both the images and flip-angle responses revealed nearly similar performances for both types of the coils. Image intensity line profiles for different orientations of the PET cable RF shields for the PET-strip coil did not show significant variations from the case without the cable shield (Fig. 5b), although there was a slight fluctuation in the S_{11} parameter.

Table 1 lists the RF power reflection (S_{11}, etc.) and transmission coefficients (S_{12}, S_{13}, etc.) for the four-channel coil in a cylindrical orientation with a phantom. Because there was a large gap between the coils, we did not implement any decoupling circuits in this study. For all the coils, the reflection coefficients were below −30 dB. The transmission coefficients between the nearest coils were approximately −20 dB, whereas they were below −25 dB between the other coils.

The transverse plane GRE image for the four-channel coil is shown in Fig. 6a. A typical flashing image intensity is clearly visible for the imaging regions near the four coils, whereas the signal intensity dropped significantly for regions between the coils. A flip-angle map for the region of interest (ROI) shown within the dotted circle in Fig. 6a is shown in Fig. 6b. For the central 60-mm-diameter imaging region, the B_1 field homogeneity was 88%, and the average flip-angle was 31°, in which the nominal flip-angle was 30°.

Table 1 S-parameters (in dB) for the four-channel coil for the phantom-loaded condition

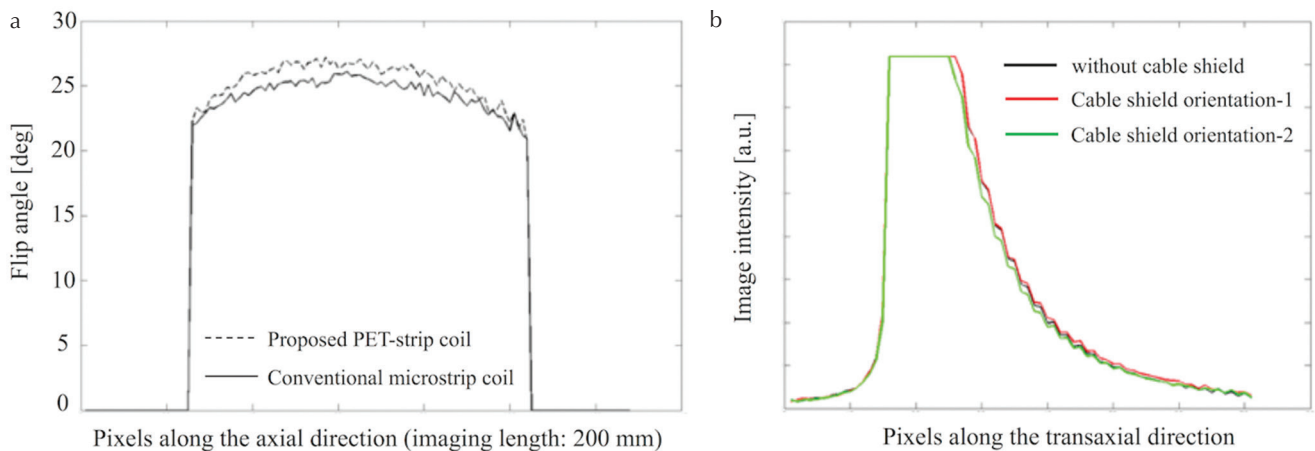|	Coil#1	Coil#2	Coil#3	Coil#4
Coil#1	S_{11} −33	S_{12} −19	S_{13} −24	S_{14} −24
Coil#2	S_{21} −17	S_{22} −29	S_{23} −19	S_{24} −35
Coil#3	S_{31} −23	S_{32} −19	S_{33} −33	S_{34} −25
Coil#4	S_{41} −24	S_{42} −36	S_{43} −25	S_{44} −32

Fig. 5 (**a**) Comparative flip-angle line profiles for the conventional and proposed single-channel coils and (**b**) comparative image intensity line profiles for the single-channel positron emission tomography (PET)-strip coil without the PET detector cable radiofrequency (RF) shield and with two different orientations of the PET detector cable RF shield.
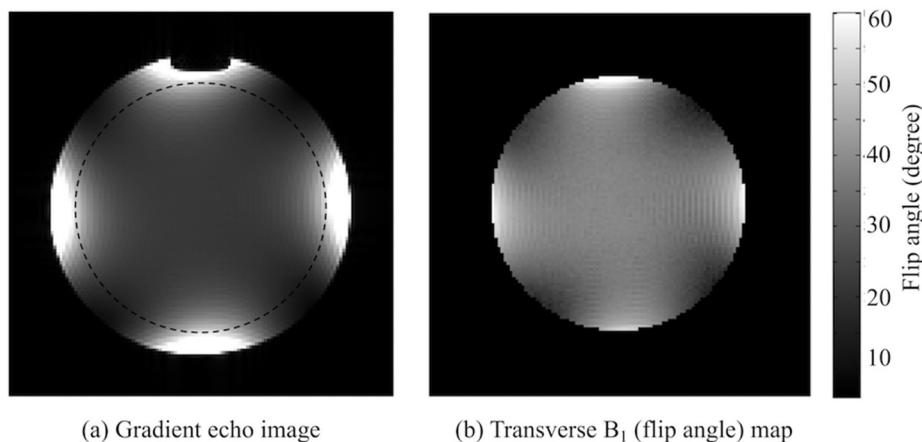

(a) Gradient echo image   (b) Transverse B_1 (flip angle) map

Fig. 6 (**a**) A transverse gradient echo (GRE) image of the four-channel positron emission tomography (PET)-strip coil. A typical flashing image intensity was observed for the region of interest (ROI) near each coil. (**b**) A transverse flip-angle distribution map is shown for the ROI within the dotted circle shown in (**a**).

Discussion

In this study, we developed a proof of concept of a combined PET-microstrip four-channel transmitting/receiving RF coil designed for a PET insert in an MRI system. Implementation of parallel RF transmission coils has mostly been observed in UHF MRI systems,[26–31,33,34] in which relatively small dimensions of RF wavelengths compared with imaging dimensions of interest require RF shimming of the transmitted field to achieve a homogeneous field distribution in the ROI, which is possible to achieve with a multi-channel transmit coil by manipulating the amplitude and phase of RF pulses in each coil. One of our goals for this work was to develop a multichannel PET-strip coil insert for a simultaneous PET/MRI investigation using a UHF MRI system, such as a 7T MRI. At a UHF, because of the large magnetic field strength, the MRI signal-to-noise ratio, image contrast, and spectral resolution increase significantly, which seems to be unachievable by other means.[25–27] Currently, we have only a 3T MRI facility, and the proposed PET-strip coil was developed for this 3T MRI system as a proof of our concept. We plan to work with a UHF MRI system in the near future.

This study implemented four PET-strip coils that covered half of the periphery of the imaging region, and the image intensity for regions in between two coils was found to be significantly low. To improve the RF performance for the whole imaging region and for PET imaging considerations, we would need to add additional PET-strip coils between the four coils, which we plan to consider in our future work. For a proof of concept, we designed a low-budget four-channel coil in this study. For the practical case of brain imaging (for example) with UHF MRI, we would require approximately 16 or more of these PET-strip coils.

Conclusion

A novel concept of a microstrip transmission line RF coil was proposed for a PET insert for MRI that combines the RF shield of the PET insert as a basic component of the coil. Compared with the conventional microstrip coil that consists of a strip conductor and a single-layer ground conductor, the proposed PET-strip coil implemented the RF shield of a PET insert detector module as the replacement for the single-layer ground conductor. A comparative study between the conventional microstrip coil and the proposed PET-strip coil revealed nearly similar performances of the two types of coils. We also investigated a four-channel PET-strip coil. As the MRI system is equipped with a single-channel transmission port, we developed a custom 4-way power divider for this study. The four-channel coil showed promising results in terms of GRE imaging and B_1 field performances. For the practical scenario of brain imaging, approximately 16 or more of these PET-strip coils would be required, and we plan to conduct that study in the near future.

Conflicts of Interest

The authors declare that they have no conflicts of interest.

References

1. Cherry SR. Multimodality imaging: beyond PET/CT and SPECT/CT. Semin Nucl Med 2009; 39:348–353.
2. Misri R. Multimodality imaging. Molecular Imaging Techniques: New Frontiers. 2013; 162–176.
3. Yankeelov TE, Abramson RG, Quarles CC. Quantitative multimodality imaging in cancer research and therapy. Nat Rev Clin Oncol 2014; 11:670–680.
4. Farwell MD, Pryma DA, Mankoff DA. PET/CT imaging in cancer: current applications and future directions. Cancer 2014; 120:3433–3445.
5. Buck AK, Nekolla S, Ziegler S, et al. SPECT/CT. J Nucl Med 2008; 49:1305–1319.
6. Mariani G, Bruselli L, Kuwert T, et al. A review on the clinical uses of SPECT/CT. Eur J Nucl Med Mol Imaging 2010; 37:1959–1985.
7. Spick C, Herrmann K, Czernin J. ^{18}F-FDG PET/CT and PET/MRI perform equally well in cancer: evidence from studies on more than 2,300 patients. J Nucl Med 2016; 57: 420–430.
8. Czernin J, Ta L, Herrmann K. Does PET/MR imaging improve cancer assessments? Literature evidence from more than 900 patients. J Nucl Med 2014; 55:59S–62S.
9. Drzezga A, Souvatzoglou M, Eiber M, et al. First clinical experience with integrated whole-body PET/MR: comparison to PET/CT in patients with oncologic diagnoses. J Nucl Med 2012; 53:845–855.
10. Catana C, Drzezga A, Heiss WD, Rosen BR. PET/MRI for neurologic applications. J Nucl Med 2012; 53:1916–1925.
11. LaForest R, Woodard PK, Gropler RJ. Cardiovascular PET/MRI: challenges and opportunities. Cardiol Clin 2016; 34:25–35.
12. Shen G, Hu S, Liu B, Kuang A. Diagnostic performance of whole-body PET/MRI for detecting malignancies in cancer patients: a meta-analysis. PLoS One 2016; 11:e0154497.
13. Pfluger T, Melzer HI, Mueller WP, et al. Diagnostic value of combined ^{18}F-FDG PET/MRI for staging and restaging in paediatric oncology. Eur J Med Mol Imaging 2012; 39:1745–1755.
14. Gatidis S, la Fougère C, Schaefer JF. Pediatric oncologic imaging: a key application of combined PET/MRI. Rofo 2016; 188: 359–364.
15. Iagaru A, Mittra E, Minamimoto R, et al. Simultaneous whole-body time-of-flight ^{18}F-FDG PET/MRI: a pilot study comparing SUVmax with PET/CT and assessment of MR image quality. Clin Nucl Med 2015; 40:1–8.

16. Brownell AL, Jenkins BG, Elmaleh DR, Deacon TW, Spealman RD, Isacson O. Combined PET/MRS brain studies show dynamic and long-term physiological changes in a primate model of Parkinson disease. Nat Med 1998; 4:1308–1312.

17. Panebianco V, Giove F, Barchetti F, Podo F, Passariello R. High-field PET/MRI and MRS: potential clinical and research applications. Clin Transl Imaging 2013; 1: 17–29.

18. Zhang X, Chen YL, Lim R, Huang C, Chebib IA, El Fakhri G. Synergistic role of simultaneous PET/MRI-MRS in soft tissue sarcoma metabolism imaging. Magn Reson Imag 2016; 34:276–279.

19. Kolb A, Wehrl HF, Hofmann M, et al. Technical performance evaluation of a human brain PET/MRI system. Eur Radiol 2012; 22:1776–1788.

20. Jung JH, Choi Y, Jung J, et al. Development of PET/MRI with insertable PET for simultaneous PET and MR imaging of human brain. Med Phys 2015; 42:2354–2363.

21. González AJ, Majewski S, Sánchez F, et al. The MINDView brain PET detector, feasibility study based on SiPM arrays. Nucl Instr Meth Phys Res A 2016; 818:82–90.

22. Nishikido F, Fujiwara M, Tashima H, et al. Development of a full-ring "add-on PET" prototype: a head coil with DOI-PET detectors for integrated PET/MRI. Nucl Instr Meth Phy Res A 2017; 863:55–61.

23. Akram MSH, Nishikido F, T Obata T, et al. Development and performance evaluation of the second prototype of a RF-coil integrated PET insert for existing 3T MRI systems. Proc Intl Soc Mag Reson Med 2017; 25.

24. Olcott P, Kim E, Hong K, et al. Prototype positron emission tomography insert with electro-optical signal transmission for simultaneous operation with MRI. Phys Med Biol 2015; 60:3459–3478.

25. van der Kolk AG, Hendrikse J, Zwanenburg JJ, Visser F, Luijten PR. Clinical applications of 7 T MRI in the brain. Eur J Radiol 2013; 82:708–718.

26. Uğurbil K. Imaging at ultrahigh magnetic fields: history, challenges, and solutions. Neuroimage 2018; 168:7–32.

27. Zhang X, Ugurbil K, Chen W. Microstrip RF surface coil design for extremely high-field MRI and spectroscopy. Magn Reson Med 2001; 46:443–450.

28. Lee RF, Hardy CJ, Sodickson DK, Bottomley PA. Lumped-element planar strip array (LPSA) for parallel MRI. Magn Reson Med 2004; 51:172–183.

29. Adriany G, Van de Moortele PF, Ritter J, et al. A geometrically adjustable 16-channel transmit/receive transmission line array for improved RF efficiency and parallel imaging performance at 7 Tesla. Magn Reson Med 2008; 59:590–597.

30. Vaughan JT, Snyder CJ, DelaBarre LJ, et al. Whole-body imaging at 7T: preliminary results. Magn Reson Med 2009; 61:244–248.

31. Shajan G, Kozlov M, Hoffmann J, Turner R, Scheffler K, Pohmann R. A 16-channel dual-row transmit array in combination with a 31-element receive array for human brain imaging at 9.4 T. Magn Reson Med 2014; 71: 870–879.

32. Bernstein MA, King KF, Zhou XJ. Handbook of MRI pulse sequences. Elsevier Academic Press, California, 2004.

33. Adriany G, Auerbach EJ, Snyder CJ, et al. A 32-channel lattice transmission line array for parallel transmit and receive MRI at 7 Tesla. Magn Reson Med 2010; 63:1478–1485.

34. Gilbert KM, Curtis AT, Gati JS, Klassen LM, Villemaire LE, Menon RS. Transmit/receive radiofrequency coil with individually shielded elements. Magn Reson Med 2010; 64:1640–1651.

35. Dregely I, Lanz T, Metz S, et al. A 16-channel MR coil for simultaneous PET/MR imaging in breast cancer. Eur Radiol 2015; 25:1154–1161.

36. Sander CY, Keil B, Chonde DB, Rosen BR, Catana C, Wald LL. A 31-channel MR brain array coil compatible with positron emission tomography. Magn Reson Med 2015; 73:2363–2375.

37. Bahl IJ, Trivedi DK. A designer's guide to microstrip line. Microwaves 1977; 16:174–182.

38. Nelatury SR, Sadiku MNO, Devabhaktuni VK. CAD Models for estimating the capacitance of a microstrip interconnect: comparison and improvisation. Proceedings of the Progress in Electromagnetics Research Symposium (PIERS), Electromagnetics Academy, Prague, Czech Republic, 2007; 18–23.

39. Stollberger R, Wach P, McKinnon G, Justich E, Ebner F. RF field mapping in vivo. Proceedings of the 7th Annual Meeting of Abstracts of the Society of Magnetic Resonance in Medicine, San Francisco, CA, USA, 1988; 106.

40. Insko EK, Bolinger L. Mapping of the radiofrequency field. J Magn Reson Ser A 1993; 103:82–85.